Materials Research
Express

PAPER • OPEN ACCESS

Qadralimb: embedded TCP actuators in silicone for grasping tasks and underwater soft robots

To cite this article: Vivek Panchal and Yonas Tadesse 2025 *Mater. Res. Express* **12** 035701

View the article online for updates and enhancements.

IOP Publishing Mater. Res. Express 12 (2025) 035701 https://doi.org/10.1088/2053-1591/adc172

Materials Research Express

CrossMark

OPEN ACCESS

RECEIVED
10 January 2025

REVISED
2 March 2025

ACCEPTED FOR PUBLICATION
17 March 2025

PUBLISHED
26 March 2025

PAPER

Qadralimb: embedded TCP actuators in silicone for grasping tasks and underwater soft robots

Vivek Panchal and Yonas Tadesse

Humanoid, Biorobotics and Smart Systems (HBS) Laboratory, Mechanical Engineering Department, Jonsson School, The University of Texas at Dallas, Richardson, TX, United States of America

E-mail: yonas.tadesse@utdallas.edu

Keywords: underwater robot, soft robot, contractile actuators, TCP muscles, artificial muscles

Supplementary material for this article is available online

Abstract

In the past few years, significant advancements have been made in soft robotics using various actuators. One notable development is the emergence of *Twisted and Coiled Polymers (TCP)* and the integration of TCP actuators in silicone. TCP artificial muscles have several advantages: they are quiet, inexpensive, exhibit low hysteresis, operate at low voltage and can be tailored for desired shapes. This research focuses on characterization of the 2-ply TCP actuators embedded in silicone and their application for a swimming robot and grasping application. Initially, the actuators were characterized for static and dynamic behaviors, considering critical parameters such as applied voltage, actuation frequency, pre-tension, resistance of the muscles, geometry and the material composition. Out of these, the first three parameters can be controlled during operation. The study determined the optimum ranges for these controllable parameters, specifically for a swimming and grasping applications. For swimming, a low-profile robotic structure with four limbs (each measuring $140 \times 60 \times 5\ \mathrm{mm}^3$) was developed that was able to swim a vertical displacement of 343 mm in 640 s. Limb actuation conditions were also optimized for grasping, demonstrating successful grasping in air and in water against gravity using a single or combined limbs. The 2-ply TCP actuators provided a strain of 12.5% at a 300 g (2.9 N) optimum load and a blocking force of 1.7 kg (16.7 N) when supplied with 225 J of electrical input energy (20 V, 0.75 A current and 15 s heating time). Notably, this soft structure with embedded TCP actuators has not been demonstrated in an underwater environment, and hence this study adds new knowledge in this area. Furthermore, FEM simulation results on a single limb under the effect of gravity was performed using ANSYS to compare with experimental results. This research has potential applications in underwater exploration and manipulation in hazardous environments.

1. Introduction

Soft robotics is relatively new and unlike conventional rigid robots, the majority of the structure of the robot is soft, where these structures are driven by either conventional actuators such as servo motors or pneumatic motors (PM) or by using non-conventional actuators like smart materials such as twisted and coiled polymers (TCP), shape memory alloys (SMA), Dielectric Elastomers (DE) etc This paper presents the design and development of one such underwater soft robot named the Quadralimb Bot that has been shown to have the ability to swim vertically. This robot has a silicone structure driven by 2-ply TCP muscles 1.15 mm in diameter and 140 mm in length, embedded in modular silicone limbs $140 \times 60 \times 5\ \mathrm{mm}^3$ that can function individually as well as in a combination with other limbs. Another aspect shown in this paper is the development of a grasping application using a single as well as a combination of two modular silicone limbs that has the potential to be integrated with the Quadralimb Bot (figure 1). The overall size of the Quadralimb Bot is 340 mm in diameter with a thickness of 12 mm. The silicone limb structure by itself as well as in a combination (Quadralimb Bot) can

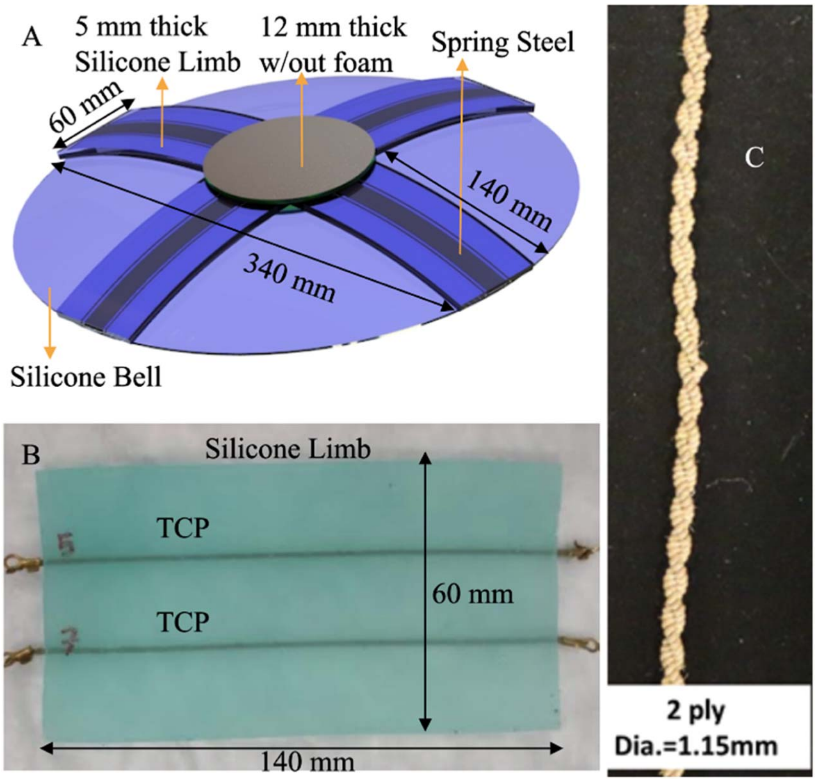

Figure 1. Embedded 2-ply TCP actuators in silicone for underwater grasping and underwater swimming robots: (A) the quadralimb bot, (B) individual silicone limb and (C) 2-ply TCP actuator.

produce various biomimetic shapes via different modes of actuation and thus are not limited to a few degrees of freedom like conventional robots.

There have been several advancements in the field of soft robotics using different actuation methods and utilizing hyperelastic materials like silicone for many potential applications. In 2017, Almubarak and Tadesse showed distinct morphing shapes like a caterpillar, elephant trunk and fish fins [1]. Lee *et al* in 2019, demonstrated the use of free sliding SMA wires as tendons that are used in a soft gripper capable of gripping a wide range of objects up to a weight of 1.5 kg [2]. In 2015, Rodrigue showed a similar smart soft composite structure actuated by SMA wires for different modes of actuation for different lengths of the soft composite [3]. In 2020, Kumar *et al* showed techniques to overcome the shortcomings of SMAs such as low force, cycle time and material nonlinearity issues [4]. Recently, 4D printing of soft robotic structures has emerged to address the challenges of multiple manual assembly processes in soft robotics [5]. Some examples include bi-stable grippers using thermal actuators that utilize ethanol vapor and carbon fiber as a heater for phase-changing artificial muscles [6, 7]. Vapor-based soft actuators are impressive in terms of actuation strain, achieving up to 140% free strain in one direction and blocking load 140 N (blocking stress 1.3 MPa), for a sample with a diameter 11.1 mm, length of 25 mm and weight of 2 g, when heated at 15 V and 1 A stimuli. However, their actuation time is slower, taking 70 s to reach peak value [8].

In 2019, Manfredi *et al* exhibited a novel soft pneumatic actuator which exhibits four degrees of freedom [9]. In 2018, Pawlowski *et al* showed a physics-based modeling of TCAs (the same as TCP) to establish a relation between the actuator and deformation of a soft robot [3]. In 2018, Tang *et al* presented a model for recovered torque in TCAs which is then used to predict the deformation under varying temperatures and validated against experimental results [10]. In 2017, Saharan and Tadesse showed a relation between the fabrication parameters and the performance of TCP muscles [11]. Wu and Tadesse explored the strain sensing principle of TCP's based on the change in their electrical resistance [12].

There have also been significant strides made in the area of soft underwater robots using several different actuators. These underwater robots in particular have been reviewed and listed in table 1 describing some of their important properties, results, and challenges. Based on our research and findings of similar work, the use of 2-ply TCP muscles embedded in a silicone structure for swimming and grasping is an unexplored area which is what makes the Quadralimb Bot and the grasping application we developed novel in nature. The overview of this research is shown in the supplementary short movie and can also be found in the following link from HBS lab YouTube Channels https://youtu.be/QYcoEAoIPMg.

Table 1. A min-review of the jellyfish like robots using various actuators for comparison with the current work.

Authors/actuator	Primary result	Primary challenge
Frame *et al* 2018 [13] Hydraulic	Conducted open water experiments showed swimming from a 5 m depth in the Atlantic Ocean. The diameter of the jellyfish was 210 mm, and the robot swimming speed was 0.14 BD s^{-1}.	Actuators are hydraulic and have low Energy Density compared to other smart materials.
Shi *et al* 2010 [14] SMA	With 24 V, obtained a top speed of 57.2 mm s^{-1} i.e., nearly 0.9 BD s^{-1}.	The rigid frame can pose a problem while navigating through orifices smaller than its dimensions.
Wang *et al* 2017 [15] SMA	Simulations show a vertical displacement of 12–16 cm in 50 s i.e., a speed of 0.1 BD s^{-1}.	Increase in volume causes a slight increase in speed for a much higher increase in cost.
Godaba *et al* 2016 [16] DE	A vertical displacement of 180 mm in 20 s is seen i.e., a speed of 1.28 BD s^{-1}.	Dielectric Elastomers take a huge voltage and might not be safe in underwater operations unless sealed.
Nir *et al* 2012 [17] Spring	The jellyfish was able to move at a speed of 8–20 mm s^{-1} in various directions.	The springs are bound to buckle both in their straight and encircled configurations.
Zhou *et al* 2016 [18] SMS	It can achieve a maximum velocity of 111 mm s^{-1} i.e., a speed of 1.63 BD s^{-1}.	The design uses a rigid bell that must envelop all the components which can cause movement issues.
Trabia *et al* 2016 [19], IMPC	Vertical displacement of 4 cm in 10 s i.e., approximated to 1 BD s^{-1}.	The force out of IMPC is not high compared to TCP.
Bartlett *et al* 2015 [20], Combustion	The robot autonomously jumped to 0.76 m high and demonstrated directional jumping up to 0.15 m where the body height is close to 0.126 m	The materials available that can be implemented in this process are limited.
Shen *et al* 2017 [21] Hydraulic	A speed of 4.2 cm s^{-1} was obtained using a straight trajectory.	There is a hysteresis effect in the actuation of the arms.
Shintake *et al* 2016 [22] DE	The jellyfish robot showed a swimming speed of 1.5 mm s^{-1} and the fish robot showed a swimming speed of 8 mm s^{-1}.	Coating the robot with electrically insulating material can greatly stiffen the structure.
Kim *et al* 2013 [23] SMA	The maximum speed of turtle-like swimming robot in a single cycle was around 0.25 body lengths s^{-1}.	The deformable behaviors of the SSC structure need to be addressed.
Cheng *et al* 2018 [24] DE	The untethered robotic jellyfish has a swim speed of up to 1 cm s^{-1} corresponding to 0.125 body lengths s^{-1}.	The power supply size needs to be reduced, and its capacity needs to be increased.
Guo *et al* 2007 [25] IPMC/SMA	The maximum floating speed obtained is 6 mm s^{-1} (0.13 body lengths/s).	The robot is tethered for power.
Joshi *et al* [26] SPC	The robot (FludoJelly) has an average speed of 160 mm s^{-1}. (10.67 BD s^{-1}).	Soft Pneumatic Composite actuators (SPC) are low in energy density.
Almubarak *et al* 2020 [27], SMA	The robot (KryptoJelly) has an instantaneous swimming speed of 60 mm s^{-1} (0.3 BD s^{-1}).	The power consumption for SMAs is high and long field operation is a challenge.
Hamidi *et al* 2020 [28] TCP (TCP_{Ag})	Poly-Saora jellyfish was able to swim 180 mm at speed of 5 mm s^{-1} i.e., a speed of 0.025 BD s^{-1}.	The power consumption for exposed TCPs is high and long field operation is a challenge.
Christianson *et al* 2019 [29], DE	The maximum swimming speed obtained for the robot during tethered operation was 1.8 mm s^{-1} and an average of 3.2 mm s^{-1} during untethered operation which corresponds to 0.02 BD s^{-1}.	Dielectric Elastomers take a huge voltage and might not be safe in underwater operations.
Matharu *et al* 2023 [30] fishing line TCP (TCP_{FL})	The Jelly-Z robot generated a velocity of 20 mm s^{-1} while carrying its own 215 g weight.	The power consumption of the fishing line TCP actuators integrated in the robot is high.
Xing *et al* 2023 [31] Piezoelectric	The bionic piezo based jellyfish best achieved was 10 mm s^{-1}.	The drive voltage of the jellyfish is high for a meaningful wireless operation.
Wang *et al* 2023 [32] Electrohydraulic	A versatile Jellyfish like robot. It's against gravity speed was up to 6.1 cm s^{-1}.	The materials used for the robot need to be improved to improve robustness, reliability, and longevity.
Matharu *et al* 2023 [33] SMA Spring	SoJel 3D printed soft robot, bell diameter of 406 mm, weight of 687 g, showed 15 mm s^{-1}. swimming speed.	Power consumption is high up to 600 W

This work is similar to prior work [1] in terms of structure and the use of 2-ply TCP. However, this work differs as it focuses testing the behavior of the TCP embedded within silicone in an underwater environment for grasping tasks and a swimming robot. Unlike the previous study's which is focused on the general behavior embedded TCPs, this work specifically targets swimming and grasping applications. It first investigates

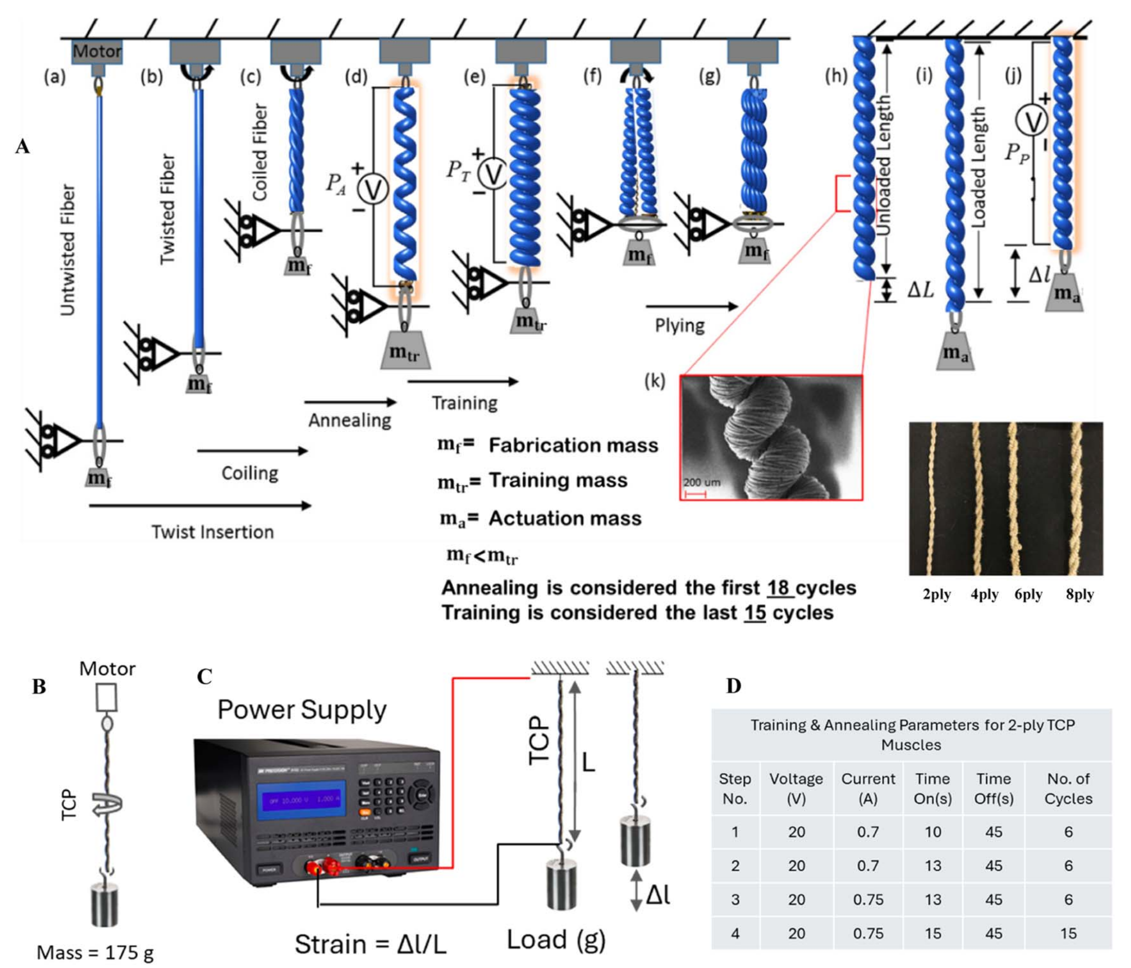

Training & Annealing Parameters for 2-ply TCP Muscles

Step No.	Voltage (V)	Current (A)	Time On(s)	Time Off(s)	No. of Cycles
1	20	0.7	10	45	6
2	20	0.7	13	45	6
3	20	0.75	13	45	6
4	20	0.75	15	45	15

Figure 2. Fabrication process of TCP muscles: (A) schematic diagram. Reprinted from [34], Copyright (2022), with permission from Elsevier, (B) schematic diagram of the twisting process of our 2-ply TCP with a DC motor and a dead weight of 175 g, (C) power supply setup for 2-ply TCP muscles, training & annealing using BK Precision 9182 programmable power supply, under a dead weight of 350 g and (D) training and annealing protocol.

parameters affecting the behavior of embedded TCPs, optimizes them for the applications, and then conducts performance tests. We used the terms swimming robot, underwater robot, and jellyfish-like soft robot interchangeably to describe our robot Quadralimb Bot in this paper.

2. Design and fabrication

2.1. Fabrication and training of TCP muscles

Firstly, 2-ply TCP muscles which are based on silver coated nylon 6,6 polymer threads are fabricated using a standard automated fabrication procedure using a DC Motor. The process has been described in [1, 34] and in figure 2, essentially the *twisting* of the fiber (typically 2.8 to 3 m long fiber) was done at 300 rpm and 175 g load, followed by *coiling* of the structure on its own, and folding into half to retain its twisted and coiled structure. The next step is *annealing* and *training* which is done by applying cyclic loading and varying heating time and current (varying power to get repeatable performance). The twisting speed and the load applied affect the performance of the muscles, too much twist at higher load makes it break, and too small load will make it snarl. The rate of twisting affects the actuation performance which can be found in prior study by Saharan and Tadesse [11]. For example, for a 2-ply TCP fabricated at a speed of 200, 600, 1000 and 1800 RPM, the strain magnitude varies 2–3%. In our 2-ply structure, when a 0.75 A current for 15 s heating time is applied at a load of 350 g, the muscle contracts and we obtain an average strain of 13.42% and an average resistivity of 0.447 Ω cm^{-1}. The mass of a single actuator including two crimps is on average 0.4 g. Following the process shown in figure 2, we made 17 such muscle samples.

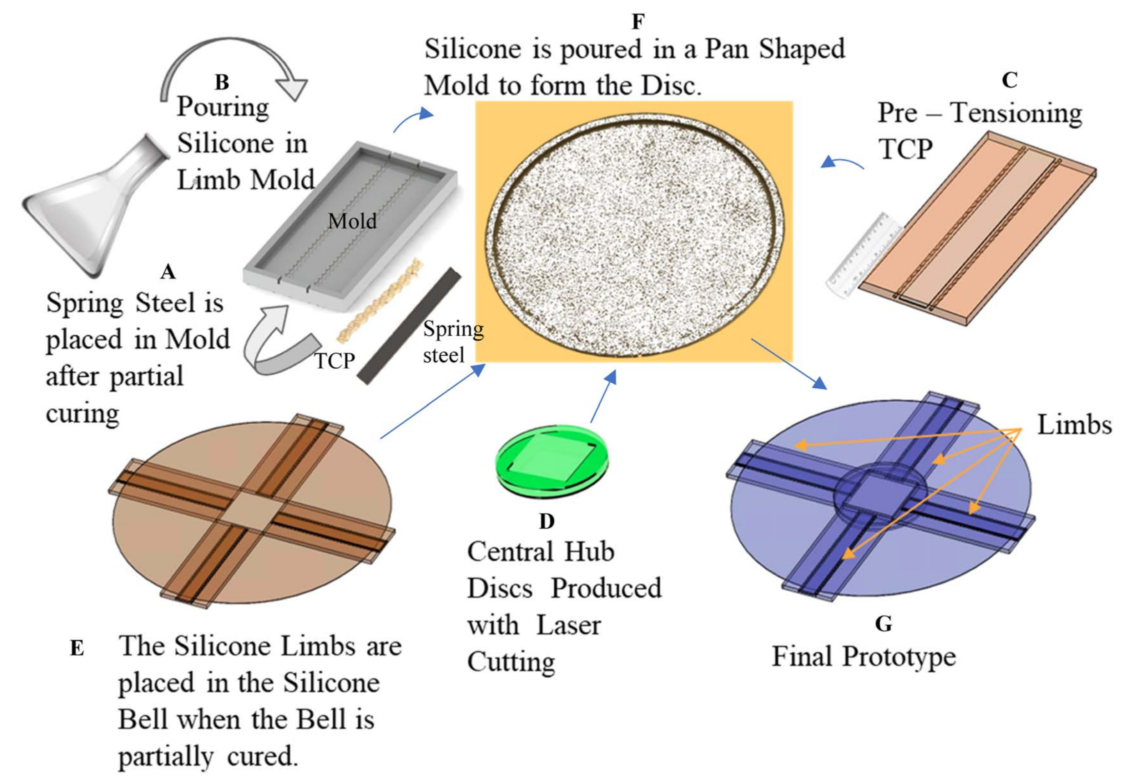

Figure 3. Fabrication process of the quadralimb with embedded TCP within silicone elastomer.

2.2. Fabrication of the quadralimb bot

Each limb is fabricated using a 3D printed mold designed specifically for a limb of a specific thickness i.e., 5 mm in this case with a length and width of 140 mm and 60 mm respectively (figure 3(A)). This mold has two additional slots in which the trained TCP muscles are placed parallel to each other at 10 mm from the central axis on opposite sides. The next step following this is the process of Casting. Ecoflex 30 is composed of two parts - A and B, which are each taken by volume (30 ml each) in a ratio of 1:1 and mixed thoroughly after which it is poured into the mold (figure 3(B)). Initially, half of the prepared volume is poured into the mold and allowed to cure for 30 min. Following this, a spring steel is placed at the center of the mold on the semi-cured silicone surface and the rest of the silicone mixture is poured into the mold. This mixture is then allowed to cure for an additional time of 3 to 4 h before it is carefully removed from the mold. Finally, the muscles are given a desired pre-tension which concludes with the first fabrication step (figure 3(C)).

The Quadralimb Bot is composed of four such silicone limbs, two polystyrene discs, a silicone bell and connecting wires. The silicone bell is fabricated in a way similar to the silicone limbs where the total volume taken is 80 ml (40 ml each of part A & B respectively). This process produces a silicone bell of thickness 0.65 mm after curing in a disc mold (figure 3(F)). Moreover, the silicone limbs are placed on the partially cured silicone bell to use the silicone itself to form a bond (glue together) during the curing process which reinforces the limbs with the bell. The two polystyrene discs that form the central hub (figure 3(D)) are designed on SolidWorks and fabricated using laser cutting. The pre-assembled silicone limbs (figure 3(C)) and the disc are then assembled with the central hub, and the entire structure is then reinforced together using fasteners (figure 3(E)). Following these procedures, the embedded muscles in the limbs are then wired for power supply after which it is ready for operation (figure 3(G)).

It is to be noted that when the TCPs are incorporated into the silicone elastomer, the silicone solidifies around the TCP muscles, creating an interface. However, it doesn't form a chemical bond with the muscles. The TCPs are secured by the elastomer network and the unique shape of the TCP muscles, which are larger in one section and smaller in another in helically wound structure (figure 1(C)).

3. Experiments and results

Several experiments have been conducted to characterize the behavior of the TCP muscles with respect to changes in critical parameters that drive these muscles in order to build and establish necessary relations to be

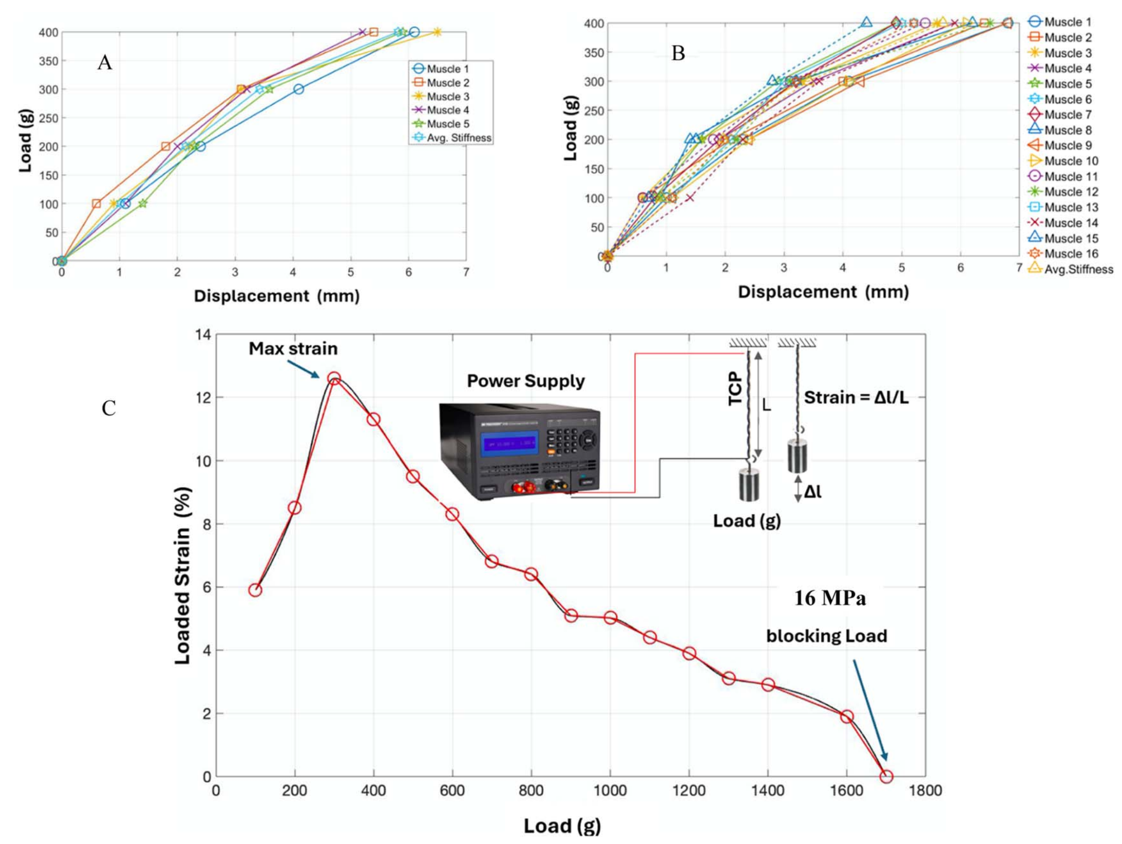

Figure 4. Characterization of 2 -ply TCP: (A) Stiffness found from 5 muscles produced using Spool 2 in a static behavior test, (B) Stiffness found from 16 muscles produced using Spool 3 in a static test and (C) Dynamic actuation test to determine the relation between change in loaded strain and applied load while supplying 20 V at 0.75 A and 15 s heating time and 45 s cooling time.

utilized in the development of two different applications i.e., swimming and grasping. Our focus is the behavior under embedded conditions and environmental conditions.

3.1. TCP muscle characterization (non-embedded condition)

The TCP muscle's stiffness is determined by a deflection test using a set of standard loads i.e., 100 g, 200 g, 300 g and 400 g. This data has been collected for muscles made using two different spools to understand the static and dynamic behavior. The average stiffness found for the two spools is 68.7 N m^{-1} and 69.24 N m^{-1} respectively (figures 4(A) and (B)). The emphasis here is that there is a consistency in the stiffness of the muscles and thus variation in this parameter can be ruled out as a reason for any variation in the behavior of the TCP muscles due to the polymeric materials.

Another important experiment was conducted to investigate the relation between change in loaded strain with respect to changing load (figure 4(C)), which is a dynamic behavior. During this experiment, the 2 -ply TCP is actuated at 0.75 A using a set voltage of 20 V for a heating time of 15 s at different loads. This corresponds to an electrical energy of 225 J. Thus, the loaded strain increases up to a certain point 300 g load with increasing load, gains a peak 12.5% strain and then starts decreasing. Another interesting result gathered from this experiment is that the muscle blocking load is at a load of 1700 g i.e. 4.85 times the weight at which it is trained and annealed. This corresponds to 16.7 N blocking force and when normalized by area, the blocking stress is 16 MPa.

3.2. TCP muscle characterization (embedded condition)

Here, we performed a series of tests on the muscles embedded in silicone with respect to changing pre-tension, the applied voltage, heating and cooling time, frequency of actuation for fast as well as slow actuation cycles in different mediums. First, we clamped at one end of the silicone with embedded TCP/Spring steel and applied electrical input power (inset of figure 5(A)). The basic relation observed in case of pre-tension is that as the pre-tension is increased, the degree of actuation also increases. Thus, when testing the actuation produced for a pre-tension of 24%, 27% and 30% at an applied voltage of 10 V for a heating time of 10 s was 2.89°, 7.82° and 13.1° respectively. The results are not shown in a plot for brevity in this article.

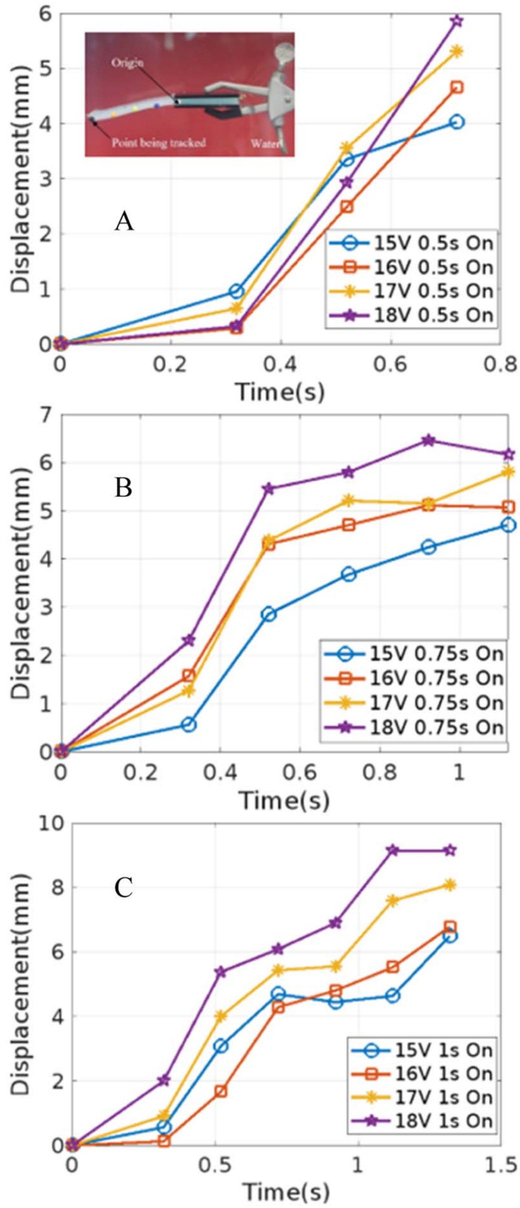

Figure 5. Characterization of 2-ply TCP (Pre-Tension at 15% and Resistance of 2 Ω) embedded in silicone to show effect of applied voltage and heating time on the angle of actuation of the silicone limb (embedded with spring steel) when tested underwater.

The next set of experiments were conducted to find optimum operational parameters for fast actuation (smaller than 10 s heating) of the silicone limb when operated underwater.

The pre-tension is fixed at 15% for each experiment described in this section from this point on unless mentioned otherwise. Moreover, each limb is embedded with a strip of spring-steel. In the next experiment, the actuation is tested for four different applied voltages i.e., 15 V, 16 V, 17 V and 18 V for a heating time of 0.5, 0.75 and 1 s. The plots in figures 5(A)–(C) show the pattern of actuation with the changing parameters. Based on these results, it was concluded that an applied voltage of 18 V or higher for a heating time of 1 s or higher can give a good degree of actuation for a swimming application.

After obtaining the previous results, another preliminary experiment was designed to investigate the voltage at which the muscles fail for a heating time of 1 s i.e., to determine an applied voltage higher than 18 V that can be used for more power for faster actuation at which the muscles can operate without breaking. The experimental setup is similar to the previous case. The initial applied voltage was 15 V and at each successful cycling, it was incremented by 1 V. The first muscle failed at 22 V for a heating time of 1 s. The second muscle failed at 23 V for a heating time of 1 s. Based on these results, an applied voltage of 18 V i.e., 15% lower than the breaking voltage, was chosen as a safe operating voltage for operation with a corresponding heating time of 1 s. Following this, the next experiments were conducted to investigate the life cycle of the muscles in an embedded condition for the operational parameters determined above.

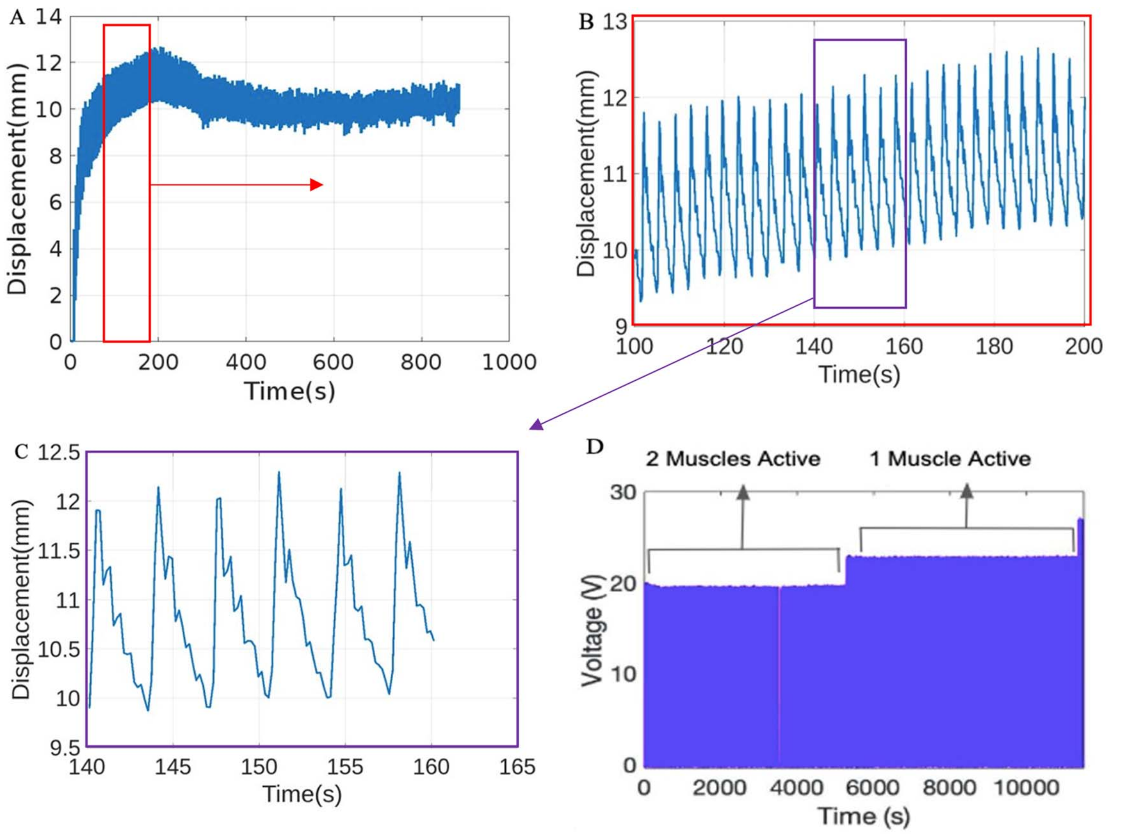

Figure 6. Life cycle pattern for 2-ply TCP(Pre-tension of 12% and resistance of 3.4 Ω.) embedded in a silicone limb at an applied voltage of 19.5 V, actuation frequency of 0.29 Hz, duty cycle of 14.3% for a total of 252 cycles that adds up to a total time period of 882 s. Actuation pattern during the entire life cycle (A), Actuation Pattern between 100 s and 200 s (B), actuation pattern between 140 s and 160 s (C) and the variation in the magnitude of voltage during the life cycle (D).

The first life cycle test was conducted at an applied voltage of 18 V, a heating time of 1 s and a cooling time of 3 s. The muscles fail after 20 cycles. After analyzing the previous results, the applied voltage was increased to 19.5 V and the heating time was reduced to 0.5 s, the cooling time was kept constant at 3 s, thus reducing the energy input. The limb was actuated until failure. The plot shown in figure 6(A) represents the actuation pattern for the first 252 cycles that adds up to a total period of 882 s. It can be clearly seen that after about 60 cycles, the actuation reduces. It so happens that after a few cycles, the TCP's begin retaining heat and the silicone acts as an insulator, because of which the muscles do not retract back to their original position and hence the degree of actuation reduces. The plots shown in figures 6(B) and (C) represent the actuation pattern for the time periods of 100 s to 200 s and 140 s to 160 s respectively. Figure 6(D) illustrates the variation in applied voltage throughout the process. In this experiment, one muscle survived 1493 cycles and the other survived 3228 cycles i.e., both muscles survive for at least 1493 cycles that adds up to a total period of 87 min.

The failure of the muscle could be due to heat buildup and delamination. The delamination of the TCP within the silicone might happen due to various factors such as the stress applied, input energy or power (voltage magnitude, duration of heating, and duty cycles), actuation frequency, and the silicone's geometry like its thickness and the size of its pores. In this study, a comprehensive study is not performed on the mechanism of delamination. However, we noticed that the biased displacement graph in the cyclic test shown in figure 6 suggests that heat builds up within the actuators embedded in the silicone. This heat could lead to the failure of the muscles, rather than the delamination. If the pre-tension is extremely high, the muscle might protrude laterally.

The last set of characterization experiments were conducted to investigate the effect of applied voltage and heating time on the degree of actuation keeping slow actuation in mind, specifically for the application of grasping. The applied voltages investigated were 8 V, 10 V and 12 V for a heating time of 1 s, 2 s and 3 s. Based on the results, the optimum operational parameters were determined to be 12 V for a minimum heating time of 3 s that can be increased to 10 s.

Figure 7. The above shown images display the swimming performance of the quadralimb Bot 3.0 for 100 cycles.

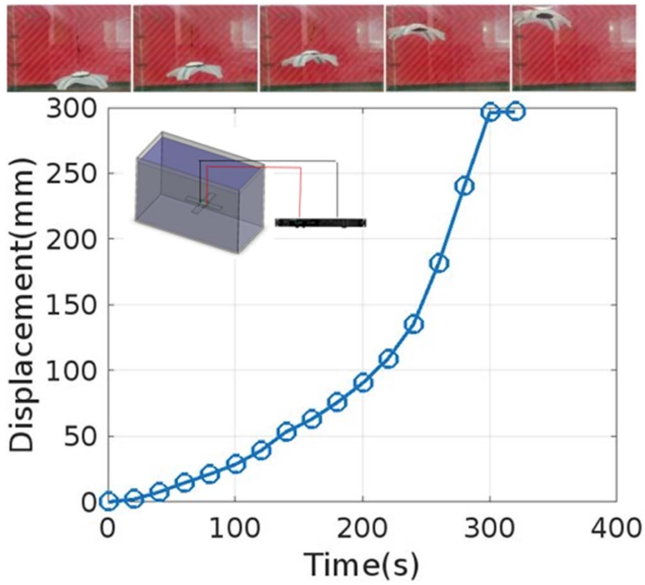

Figure 8. The plot above represents the vertical displacement of the quadralimb Bot 3.0 for 100 cycles. The total vertical displacement obtained in this experiment was 300 mm at an applied voltage of 19.5 V, frequency of 0.31 Hz, duty cycle of 28% (Prototype Mass – 372 g, Diameter – 340 mm, Average Strain of 2-ply TCP actuators used – 11%, Net Resistance of Quadralimb Bot – 1.37 Ohm, Power Supplied - 260 W).

3.3. Vertical swimming tests on quadralimb

In this section, we present the results for swimming tests which were carried out using the experimental setup presented in figure 7. The first experimental setup with prototype 1.0 was supplied with an applied voltage of 15 V for a heating time of 1 s and a cooling time of 3 s for 100 cycles which is a total actuation period of 400 s. All the limbs were actuated at the same time with the same amplitude of voltage and phase angle. This test was carried out in a water tank of size 70 gallons filled with water at room temperature. The Quadralimb Bot traveled a net displacement of 45.6 mm. Thus, since the displacement and velocity were very low, it was decided to optimize the structure & operational parameters to improve performance.

In Prototype 2.0, a circular silicone bell was added at the center of the Bot using simple cable harnessing to reinforce the silicone bell to the silicone limbs. The experimental setup is the same as the previous case. The Bot traveled a net displacement of 110.32 mm at an applied voltage of 18 V for a heating time of 0.5 s and a cooling time of 2.5 s. Thus, the results obtained were a significant improvement over the previous results, however it was decided to further optimize the operational parameters and the structure of the prototype to improve the performance.

The third experimental setup with prototype 3.0, its progression of swimming and its displacement versus time plot can be seen in figures 7 and 8. Prototypes 3.0 and 4.0 were fabricated using the process described in section 2.2 where the primary difference from Prototype 2.0 is the method of fastening the silicone limbs to the bell. The Bot was supplied with an applied voltage of 19 V for a heating time of 0.7 s and a cooling time of 2.5 s for 100 cycles that amounts to a total period of 320 s. The Bot traveled with a net displacement of 300 mm. Thus, it is a significant improvement over the previous results. Following this, it was decided to fabricate another prototype and test it at the same parameters to check the repeatability of the experiment.

The fourth experimental setup with prototype 4.0, its snapshot of the swimming and vertical displacement versus time plot can be seen in figures 9 and 10. The Bot was actuated with an applied voltage of 19 V for a

Figure 9. The above shown images display the swimming verticailly up and down of the Quadralimb Bot 4.0 for 200 cycles.

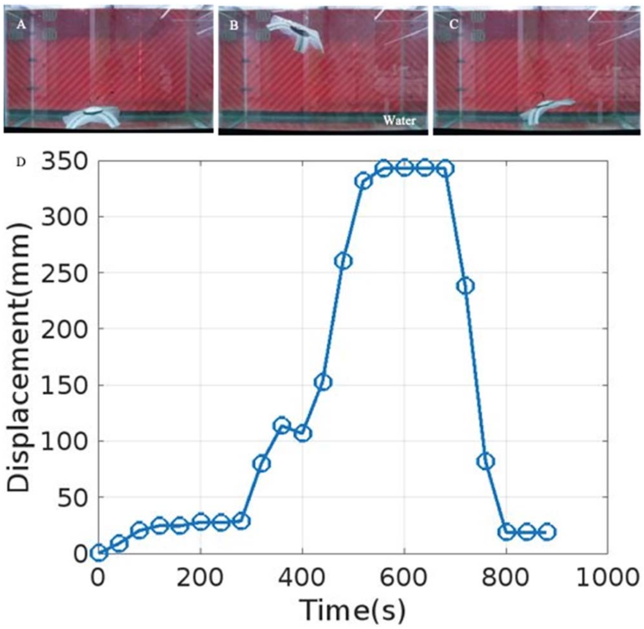

Figure 10. The vertical displacement of the quadralimb Bot 4.0 for 200 cycles. The total vertical displacement obtained in this experiment was 343 mm in 640 s at an applied voltage of 19.5 V, frequency of 0.31 Hz, duty cycle of 28% (Prototype Mass −363 g, Diameter −343 mm, Average Strain of 2-ply TCP Actuators used −10.56%, Net Resistance of Quadralimb Bot −1.39 Ohm, Power Supplied −258.4 W).

heating time of 0.7 s and a cooling time of 2.5 s for 200 cycles, this corresponds to a total time of 640 s. Initially, the Bot was actuated for 100 cycles. After the 100 cycles ended, the Bot was actuated for another 100 cycles after a slight delay which caused a loss of inertia mid-way in the Bot's vertical displacement. The Bot traveled a total vertical displacement of 343 mm. Thus, even though the displacement improved, the velocity decreased as compared to the previous experiment. However, primarily this experiment shows that these results are repeatable. Thus, the operational parameters can be further optimized to achieve better performance in the future.

3.4. Grasping tests

In this section, we present the test results for different grasping using a single limb in air as well as a combination of two such limbs in water using objects of varying sizes, shapes, and weights. The aim here is to develop a grasping application that can work independently as well as one that can be integrated with the Quadralimb Bot. The initial experiments were done to test the ability of a single limb to grasp objects of varying geometries and weights in two different orientations, curling and handling the object. Here, the objects vary in geometry from a cylindrical to a cuboidal shape and vary in weight from 2.5 g to 25 g. The objects have been grasped and held against gravity. These experiments use an applied voltage of 12 V for a minimum heating time of 3 s. Different objects grasped by the limb can be seen in figures 11(A)–(C). The initial configuration, the intermediate shapes when we turn on the power supply and the final actuated shapes are shown in the three columns in the figure. Figure 11(D) shows an object that is mounted on the structure and holding it effectively when actuated. In this case, the curvature was high and there is no issue of slipping from the grip as the object is on the top of the skin.

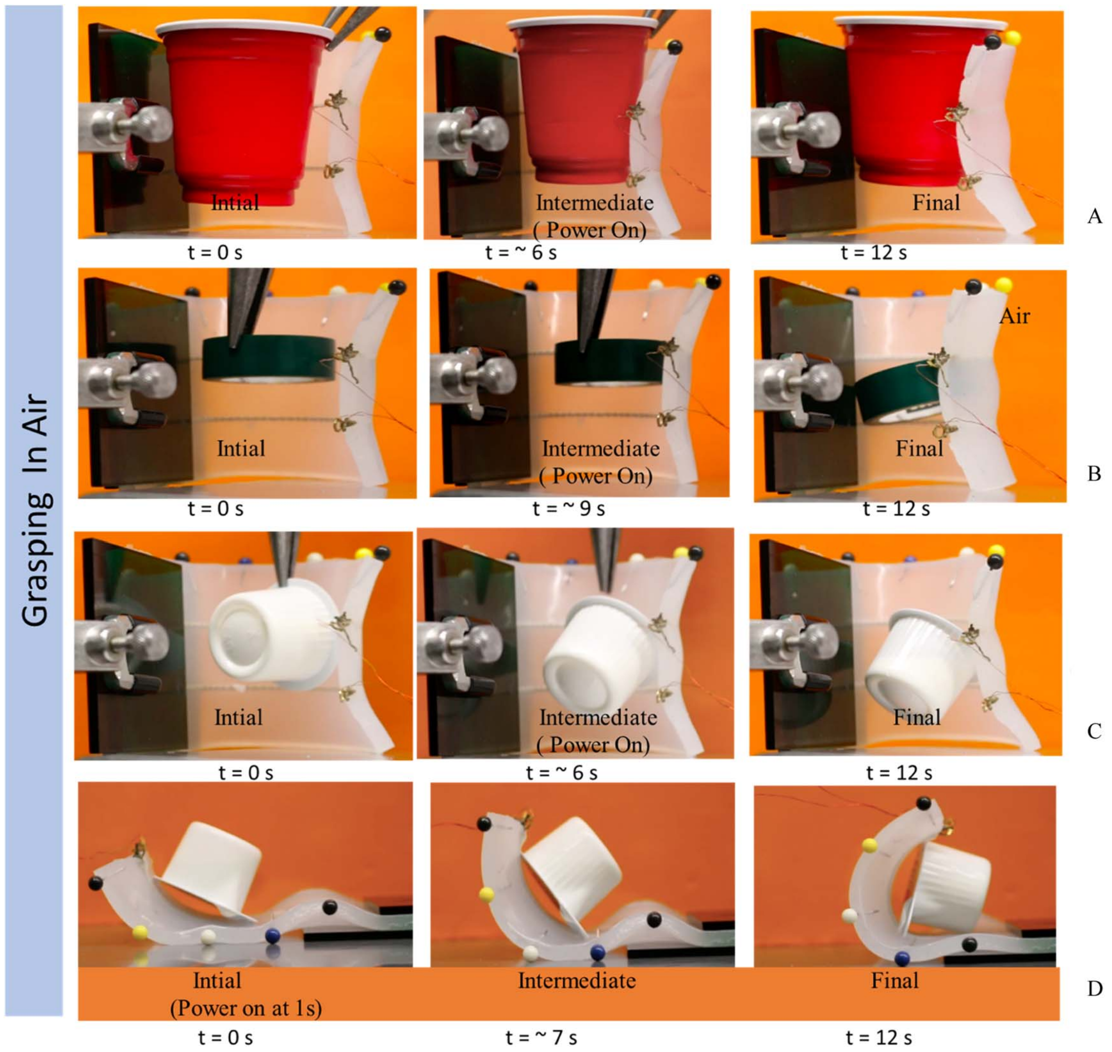

Figure 11. Vertical grasping of objects in air ((A) to (C), the top three rows), gravity is vertically downward and horizontal grasping of objects by keeping objects on the top of the skin with a single limb is shown at the bottom row (D). The intermediate steps shown in the second column for each row indicate the power on state (actuating the muscles) and the time variation is because we didn't focus on the powering time (on time), rather the holding of the object is the main goal of the experiment.

It was then decided to test the weight holding capacity of the limb in air while in the vertical orientation against gravity as can be seen in 11(A). A red plastic cup is used here as a base weight. To test different weights, the cup is filled with a standard screw that weighs 1.832 g, adding two units of screws after each test. These tests were conducted until the muscle fails. The experiment failed at a weight of 37 g and the maximum weight the limb was able to grasp without failing was 35 g. The input power supplied to the muscles was on average 43.5 W (applied voltage of 12 V and current of 3.63 A). The pre-tension in the muscles was 20% and the resistance of the two muscles embedded was 2.53 Ω.

The previous experiments were conducted in the air and the next set of experiments were conducted to test the ability of a single limb as well as a combination of two limbs to grasp different objects in water against gravity. The grasping for one of the objects has been shown in figure 12(A). Following this, a combination of two limbs has been shown to grasp a glass of mass 82 g (figure 12(B)). It is important to note here that the limbs grasp and hold the objects against gravity without any support. These experiments use an applied voltage of 12 V for a minimum heating time of 3 s that can be extended up to 10 s as needed. An experiment to test the weight holding capacity of limbs in water was not conducted due to challenges with respect to the experimental setup at the time.

4. Theoretical study

4.1. FEM simulations

The limb was modeled on ANSYS using the Yeoh 3rd order model which is frequently used for hyperelastic materials like silicone equation (1). The material constants are defined as C1 = 12738 Pa, C2 = 709.29 Pa, C3 = −0.4565 Pa. The material constants used are derived from the work done by Hamidi and Tadesse in 2020

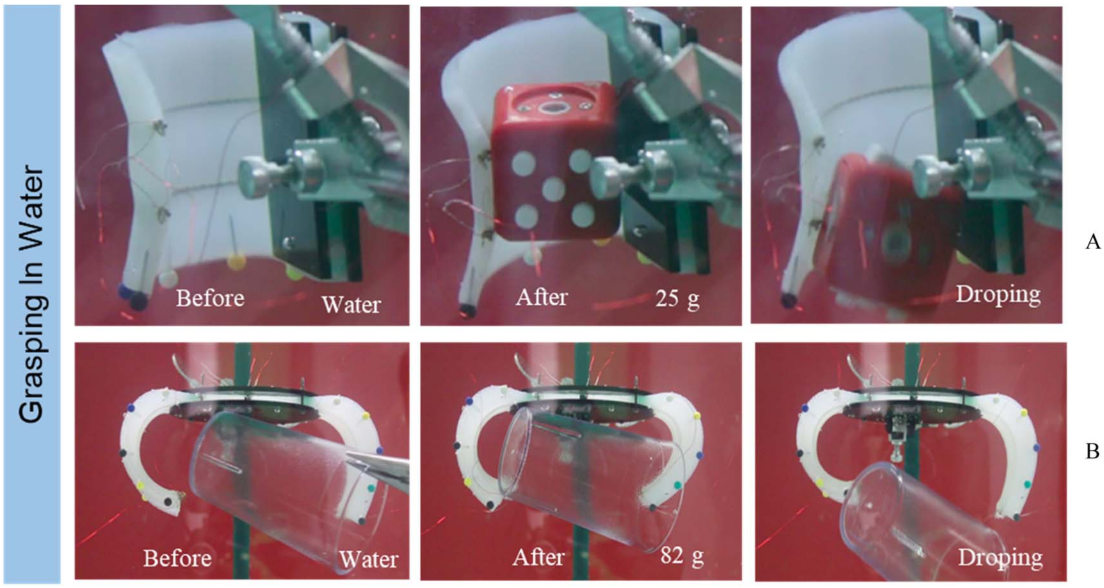

Figure 12. Grasping of objects in water using a single limb at top (A) and two limbs bottom (B), demonstrating the capture and release of two objects in water.

[35]. The simulation is done using ANSYS for limbs of three different lengths i.e., 100 mm, 120 mm, and 140 mm.

$$W = \sum_{i=1}^{n} C_i (I - 3)^i \tag{1}$$

W is the strain energy and *Ci* is the material constant, and I is the strain invariant.

The vertical deflection (VD) obtained for each case using the simulation deviates slightly from the experimental results as can be seen in figures 13(A)–(F). The maximum error obtained i.e., 11% is in the second case where the experimental deflection is 42 mm, and the simulated deflection is 47 mm. This can be clearly seen in figures 13(B) and (E). These basic simulations help us to establish a relation between simulation and experiment with respect to behavior of the silicone limbs under gravity with the potential to extend these simulations to different types of actuations of the limbs in the future.

4.2. Simulations in air

The next set of simulations conducted were to test the effect of forces applied along the silicone limb in the same orientation and direction as applied by the embedded TCP muscles when tested experimentally. The Yeoh 3rd order model was used to model the limb that is the same as described in section 4.1. The fixed support, the effect of gravity, the forces applied, and the meshing can be seen in figures 14(A)–(D). The vertical and horizontal displacement are tested for five different forces i.e. 0 N, 0.5 N, 1 N, 2 N and 3.5 N shown in figures 14(E)–(I). These are the loads at which the muscles are trained and annealed, and it can be clearly seen in figure14(I) that the limb almost bends completely at this load. These simulations are conducted for air and without applying spring steel. As expected, as the load increases, the bending magnitude increases as seen in the results. More simulation will be conducted in the future considering the spring elements as well as varying the surrounding medium.

5. Summary and conclusion

To summarize, this paper introduced a soft underwater robot, the Quadralimb Bot that was actuated using embedded 2-ply TCP muscles and spring steel in a soft silicone limb. Thus, all in all more than 90% of the structure by volume is composed of soft structures and it has a very thin structure (12 mm in thickness with embedded TCP muscles) compared to other structures presented. Four different prototypes were fabricated to carry out an experimental swimming study. The best results obtained in terms of displacement were for the third and fourth prototypes where the Quadralimb Bot was able to travel by a vertical displacement of 300 mm in 320 s (figure 8) and 343 mm in 640 s (figure 10) respectively. Several similar underwater soft robots have been made which have been described in table 1 where it has been shown that different forms of actuation have been used

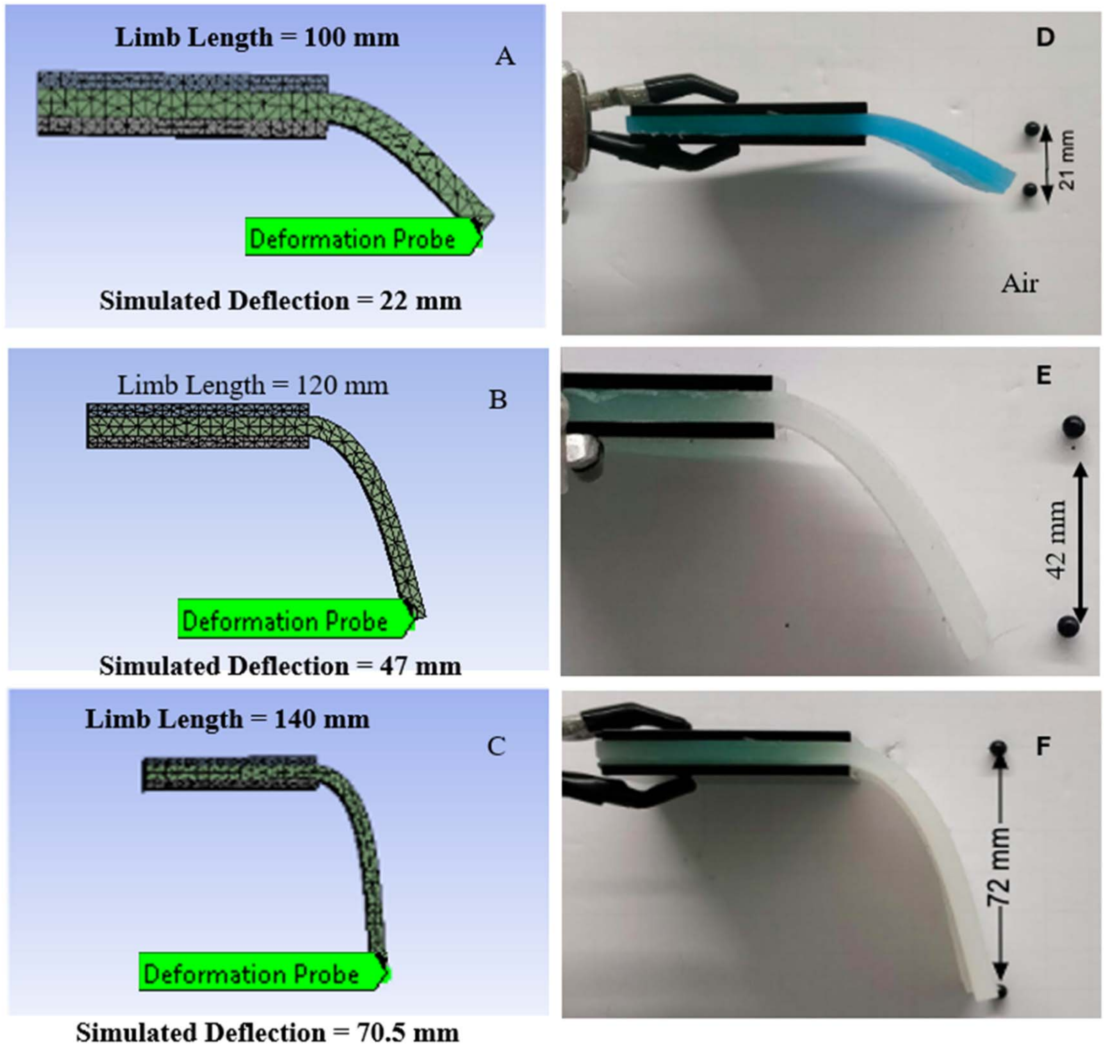

Figure 13. Simulations to show effect of gravity on a silicone limb in air shown in (A)–(C) which has been verified by experiments shown in (D)–(F) respectively.

such as SMA's, hydraulic and pneumatic actuators, DE's, IPMC's, which makes the use of 2-ply TCPs embedded in silicone for actuation one of a kind. Moreover, 2-ply TCP actuators are quiet, inexpensive, have a high energy density (5.3 kW kg^{-1} [1, 36]) and can be tailored using various parameters to produce desired shapes depending on the application.

A test on the 2-ply TCP showed that a strain of 12.5% at an optimum load of 330 g (2.9 N) and a maximum blocking force of 1.67 kg (16.7 N) when energized with 225 J of electrical energy. The paper also introduced a grasping application (figure 11) using the silicone limbs embedded with 2-ply TCP muscles. A single limb as well as a combination of two limbs were shown to grasp five objects, typically cylindrical and cuboidal shapes, and where the maximum grasping weight in air was 35 g (0.34 N). Even though the load capacity is low, the structure can conform to irregular objects for delicate grasping and holding. Moreover, the research has shown various characterization results for the 2-ply TCP muscles with respect to critical parameters like the pre-tension, applied voltage, heating time and the frequency of actuation for both slow as well as fast actuation. These characterization tests helped in finding the optimum parameters for the swimming operation of the Quadralimb Bot as well as for the grasping application that can be potentially integrated with the Quadralimb Bot in the future. Another important part of this paper is the modelling of the silicone limbs under the effect of gravity using ANSYS using Yeoh's 3rd order model to develop a relation between experiment and simulation (figures 13 and 14). With further work, these simulations can be extended to replicate different modes of actuation for a single limb as well as the Quadralimb Bot.

Our primary purpose here was to create a biomimetic jellyfish like soft robot that utilizes 2-ply TCP muscles for swimming and grasping applications. Along with understanding, characterizing, and optimizing critical parameters that significantly affected the 2-ply TCP's operation keeping both slow and fast actuation in mind. We also focused on developing a soft robotic structure inspired by a jellyfish that could harness the actuation

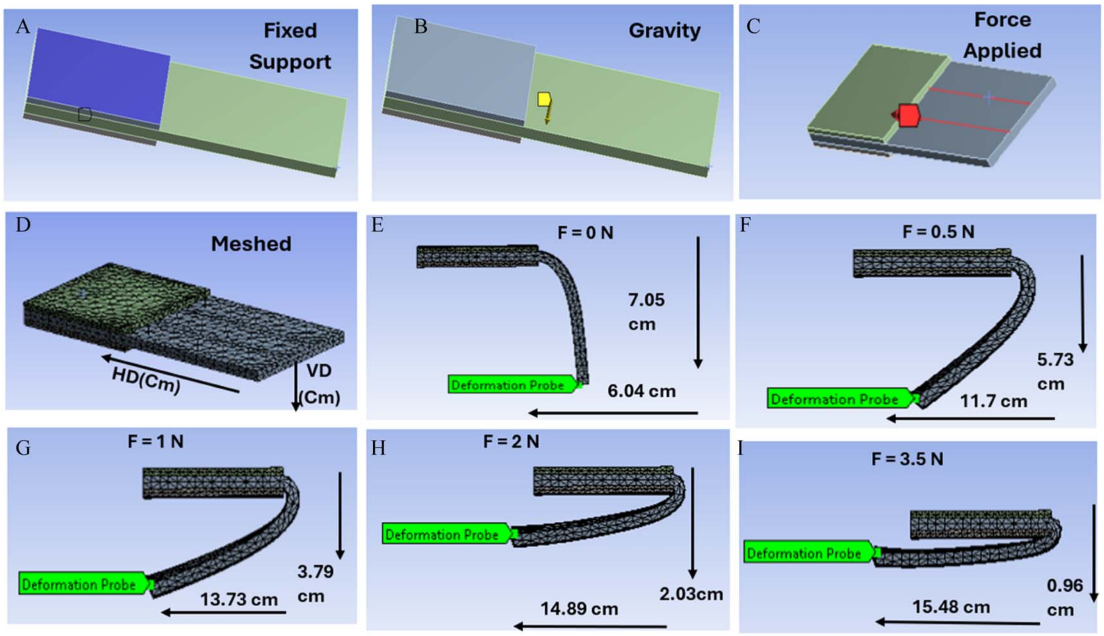

Figure 14. Simulations to show effect of applied forces on a silicone limb under gravity in air. The simulated results for the horizontal displacement shown are numerically similar for experiment in air (VD = Vertical Displacement and HD = Horizontal Displacement).

produced by the 2-ply embedded TCPs in water to its full potential. Thus, along with a change in critical parameters, an improvement in the structure of the robot also had an impact in delivering a better performance from Prototype 1.0 to Prototype 3.0 and Prototype 4.0.

Our primary aim for future work will be to further optimize the critical parameters and the robotic structure to improve performance with respect to swimming and make it quantifiable as well as multi-directional. Moreover, we aim to incorporate 3D and 4D Printing for the fabrication of our soft robots, similar to what has been shown by Mohammadi *et al* in 2023 [6] and Zolfagharian *et al* in 2023 respectively [7]. Such techniques can provide a lot of additional consistency and uniformity in the structure of the soft robots in addition to making the entire process more streamlined. Another important step would be to introduce an onboard battery, wireless communication and make the robot completely untethered. The addition of an onboard camera along with different sensors to monitor environmental parameters will be a significant potential improvement. Another aim we have in mind is to integrate the swimming and grasping functions and give the Quadralimb Bot the ability to grasp different objects in its environment. Such a robot has several practical applications such as the exploration of toxic and dangerous environments where humans cannot enter, exploration of constricted areas where traditional ROV's cannot be maneuvered, or they can be mounted in underwater vehicles as an attachment for grasping certain items They can also be used in the study of aquatic organisms due to their soft nature and quiet operation.

Acknowledgments

We would like to acknowledge the support of the Office of Naval Research.

Data availability statement

The data cannot be made publicly available upon publication because the cost of preparing, depositing and hosting the data would be prohibitive within the terms of this research project. The data that support the findings of this study are available upon reasonable request from the authors.

Supplementary movie

The overview of the Quadralimb, grasping in air, in water and swimming behaviors of the different prototypes can be found in the supplementary file submitted. This video shows the actuation of a structure consisting of

2-ply TCP muscles embedded within silicone skin referred to as single limb. The single limb is used to make a gripper using two structures and grasping of object in air and water are shown. In addition, the Quadralimb Bot characterizations are shown, and we evaluated four prototypes experimentally.

ORCID iDs

Yonas Tadesse https://orcid.org/0000-0001-6606-7089

References

[1] Almubarak Y and Tadesse Y 2017 Twisted and coiled polymer (TCP) muscles embedded in silicone elastomer for use in soft robot *International Journal of Intelligent Robotics and Applications* **1** 352–68
[2] Lee J-H, Chung Y S and Rodrigue H 2019 Long shape memory alloy tendon-based soft robotic actuators and implementation as a soft gripper *Sci. Rep.* **9** 11251
[3] Pawlowski B, Sun J, Xu J, Liu Y and Zhao J 2018 Modeling of soft robots actuated by twisted-and-coiled actuators *IEEE/ASME Trans. Mechatron.* **24** 5–15
[4] Kumar D, Daudpoto J and Chowdhry B S 2020 Challenges for practical applications of shape memory alloy actuators *Mater. Res. Express* **7** 073001
[5] Bodaghi M, Wang L, Zhang F, Liu Y, Leng J, Xing R, Dickey M D, Vanaei S, Elahinia M and Hoa S V 2024 4D printing roadmap *Smart Mater. Struct.* **33** 113501
[6] Mohammadi M, Kouzani A Z, Bodaghi M, Xiang Y and Zolfagharian A 2023 3D-printed phase-change artificial muscles with autonomous vibration control *Adv. Mater. Technol.* **8** 2300199
[7] Zolfagharian A, Lakhi M, Ranjbar S, Sayah Irani M, Nafea M and Bodaghi M 2023 4D printing parameters optimisation for bi-stable soft robotic gripper design *Journal of the Brazilian Society of Mechanical Sciences and Engineering* **45** 224
[8] Miriyev A, Stack K and Lipson H 2017 Soft material for soft actuators *Nat. Commun.* **8** 596
[9] Manfredi L, Putzu F, Guler S, Huan Y and Cuschieri A 2019 4 DOFs hollow soft pneumatic actuator–HOSE *Mater. Res. Express* **6** 045703
[10] Tang X, Liu Y, Li K, Chen W and Zhao J 2018 Finite element and analytical models for twisted and coiled actuator *Mater. Res. Express* **5** 015701
[11] Saharan L and Tadesse Y 2016 Fabrication parameters and performance relationship of twisted and coiled polymer muscles *ASME 2016 Int. Mechanical Engineering Congress and Exposition* (American Society of Mechanical Engineers) (https://doi.org/10.1115/IMECE2016-67314)
[12] Wu L and Tadesse Y 2017 Modeling of the electrical resistance of TCP muscle *IMECE 2017* (ASME) (https://doi.org/10.1115/IMECE2017-72065)
[13] Frame J, Lopez N, Curet O and Engeberg E D 2018 Thrust force characterization of free-swimming soft robotic jellyfish *Bioinspiration & Biomimetics* **13** 064001
[14] Shi L, Guo S and Asaka K 2010 A novel jellyfish-like biomimetic microrobot *IEEE/ICME Int. Conf. on Complex Medical Engineering* (IEEE) (https://doi.org/10.1109/ICCME.2010.5558830)
[15] Wang Z, Lin X, Feng X, Qin H and Xu S 2017 A motion simulation of bionic jellyfish based on shape memory alloy *2017 36th Chinese Control Conf. (CCC)* (IEEE) (https://doi.org/10.23919/ChiCC.2017.8028402)
[16] Godaba H, Li J, Wang Y and Zhu J 2016 A soft jellyfish robot driven by a dielectric elastomer actuator *IEEE Robotics and Automation Letters* **1** 624–31
[17] Nir S, Ruchaevski I, Shraga S, Shteinberg T and Moshe B B 2012 A jellyfish-like robot for mimicking jet propulsion *2012 IEEE 27th Convention of Electrical and Electronics Engineers in Israel* (IEEE) (https://doi.org/10.1109/EEEI.2012.6377056)
[18] Zhou Y, Jin H, Liu C, Dong E, Xu M and Yang J 2016 A novel biomimetic jellyfish robot based on a soft and smart modular structure (SMS) *2016 IEEE Int. Conf. on Robotics and Biomimetics (ROBIO)* (IEEE) (https://doi.org/10.1109/ROBIO.2016.7866406)
[19] Trabia S, Shen Q, Stalbaum T, Hunt R, Hwang T and Kim K 2016 Numerical and experimental investigation of a biomimetic robotic jellyfish actuated by ionic polymer-metal composite *2016 13th Int. Conf. on Ubiquitous Robots and Ambient Intelligence (URAI)* (IEEE) (https://doi.org/10.1109/URAI.2016.7625737)
[20] Bartlett N W, Tolley M T, Overvelde J T, Weaver J C, Mosadegh B, Bertoldi K, Whitesides G M and Wood R J 2015 A 3D-printed, functionally graded soft robot powered by combustion *Science* **349** 161–5
[21] Shen Z, Na J and Wang Z 2017 A biomimetic underwater soft robot inspired by cephalopod mollusc *IEEE Robotics and Automation Letters* **2** 2217–23
[22] Shintake J, Shea H and Floreano D 2016 Biomimetic underwater robots based on dielectric elastomer actuators *2016 IEEE/RSJ Int. Conf. on Intelligent Robots and Systems (IROS)* (IEEE) (https://doi.org/10.1109/IROS.2016.7759728)
[23] Kim H-J, Song S-H and Ahn S-H 2012 A turtle-like swimming robot using a smart soft composite (SSC) structure *Smart Mater. Struct.* **22** 014007
[24] Cheng T, Li G, Liang Y, Zhang M, Liu B, Wong T-W, Forman J, Chen M, Wang G and Tao Y 2018 Untethered soft robotic jellyfish *Smart Mater. Struct.* **28** 015019
[25] Guo S, Shi L, Ye X and Li L 2007 A new jellyfish type of underwater microrobot *2007 Int. Conf. on Mechatronics and Automation* (IEEE) (https://doi.org/10.1109/ICMA.2007.4303595)
[26] Joshi A, Kulkarni A and Tadesse Y 2019 FludoJelly: experimental study on jellyfish-like soft robot enabled by soft pneumatic composite (SPC) *Robotics* **8** 56
[27] Almubarak Y, Punnoose M, Maly N X, Hamidi A and Tadesse Y 2020 KryptoJelly: a jellyfish robot with confined, adjustable pre-stress, and easily replaceable shape memory alloy NiTi actuators *Smart Mater. Struct.* **29** 075011
[28] Hamidi A, Almubarak Y, Rupawat Y M, Warren J and Tadesse Y 2020 Poly-Saora robotic jellyfish: swimming underwater by twisted and coiled polymer actuators *Smart Mater. Struct.* **29** 045039
[29] Christianson C, Bayag C, Li G, Jadhav S, Giri A, Agba C, Li T and Tolley M T 2019 Jellyfish-inspired soft robot driven by fluid electrode dielectric organic robotic actuators *Frontiers in Robotics and AI* **6** 126

[30] Matharu P S, Gong P, Guntaka K P R, Almubarak Y, Jin Y and Tadesse Y T 2023 Jelly-Z: swimming performance and analysis of twisted and coiled polymer (TCP) actuated jellyfish soft robot *Sci. Rep.* **13** 11086

[31] Xing J, Jin W, Yang K and Howard I 2023 A bionic piezoelectric robotic jellyfish with a large deformation flexure hinge *IEEE Trans. Ind. Electron.* **70** 12596–605

[32] Wang T, Joo H-J, Song S, Hu W, Keplinger C and Sitti M 2023 A versatile jellyfish-like robotic platform for effective underwater propulsion and manipulation *Sci. Adv.* **9** eadg0292

[33] Matharu P S, Wang Z, Costello J H, Colin S P, Baughman R H and Tadesse Y T 2023 SoJel–A 3D printed jellyfish-like robot using soft materials for underwater applications *Ocean Eng.* **279** 114427

[34] Hamidi A and Tadesse Y 2022 Manufacturing highly elastic skin integrated with twisted and coiled polymer muscles: toward 4D printing *Smart Materials in Additive Manufacturing* ed M Bodaghi and A Zolfagharian (Elsevier) 311–27

[35] Hamidi A and Tadesse Y 2020 3D printing of very soft elastomer and sacrificial carbohydrate glass/elastomer structures for robotic applications *Mater. Des.* **187** 108324

[36] Haines C S, Lima M D, Li N, Spinks G M, Foroughi J, Madden J D, Kim S H, Fang S, Jung de Andrade M and Göktepe F 2014 Artificial muscles from fishing line and sewing thread *Science* **343** 868–72